THE ASTROPHYSICAL JOURNAL, **308**: 337–346, 1986 September 1

C^{+2} ELECTRON TEMPERATURES IN PLANETARY NEBULAE

JAMES B. KALER
Astronomy Department, University of Illinois
Received 1985 December 26; accepted 1986 February 7

ABSTRACT

Electron temperatures are calculated for 30 planetary nebulae from the flux ratios of the C III] λ1909 and C II λ4267 lines, both of which are produced in the C^{+2} zone of the nebula. These temperatures correlate much better with optical [O III] temperatures than they do with those derived from [N II], except for low central star temperatures, for which the lower ionization stages dominate. However, as calculated from currently available atomic parameters, the $T_e(C^{+2})$ average $\sim$2000 K lower than T_e[O III]. The two can be brought into agreement either by decreasing the target area of the C^{+2} ($2s^2\ ^1S$–$2s2p\ ^3P$) transition or by increasing the $C^+(\lambda4267)$ effective recombination coefficient by about a factor of 4, which would help to reconcile the abundance discrepancies derived from optical and ultraviolet line intensities. Given the complexity of the recombination problem, the latter course would seem the most likely, although a combination of errors cannot be ruled out. Electron temperatures from C^{+2} are also calculated from the application of this empirical correction factor, which are then in reasonable accord with T_e[O III], although some systematic differences still appear to be present. Comparison of these two temperatures for IC 4997 shows the density of this unusual nebula to be $8.6 \pm 1.9 \times 10^5$ cm^{-3}.

Subject heading: nebulae: planetary

I. PURPOSE

Carbon abundances are of great importance to the study of planetary nebulae and to that of their predecessors, the AGB stars, since this element, like helium and nitrogen, is dredged to the surface of the giant before ejection of the nebula: see Kaler (1985) for a review of the subject. Carbon presents a particular problem, however, first because the optical lines are produced by recombination, for which the cascade matrix has never been fully studied, and second because the collisionally excited ultraviolet lines are very sensitive to electron temperature. The result is a serious discrepancy between carbon compositions—both ionic and total—derived from the optical and UV parts of the spectrum, well documented by Harrington *et al.* (1980, 1982); Aller, Keyes, and Czyzak (1981*a*); Aller *et al.* (1981*b*); Shields *et al.* (1981); and in a series of papers by Barker (1982, 1983, 1984, 1985, 1986). The purpose of this study is to help resolve this problem by using the C III] λ1909 and C II λ4267 flux ratios to test the optical line formation mechanism, and to find the electron temperatures appropriate to the C^{+2} zones in the nebulae.

II. THE C III] λ1909–C II λ4267 FLUX RATIO

a) Theory

The C III] λ1909 intercombination doublet is caused chiefly by collisional excitation of the $2s2p\ ^3P$ term of the C^{+2}, followed by radiative decay. The collisional excitation rate is given by Flower and Launay (1973) as

$$q_{ij} = \frac{8.63 \times 10^{-8}}{\tilde{\omega}_i \sqrt{t}} \gamma e^{-E_{ji}/kT} , \qquad (1)$$

where $t = 10^{-4}$ times the electron temperature T_e, and $\tilde{\omega}_i = 1$. From Harrington *et al.* (1980), $\gamma = 1.05t^{-0.042}$. The transition probability determined by Nussbaumer and Storey (1978) shows that the radiative decay rate is orders of magnitude faster than the collisional deexcitation rate, which can then be ignored. Consequently, the volume emissivity for the line can be written as

$$E_c(\lambda1909) = 9.43 \times 10^{-19} t^{-0.54} e^{-7.5364/t} N(C^{+2}) N_e , \qquad (2)$$

where $N(C^{+2})$ and N_e are the ionic and electron densities respectively.

Some component of the λ1909 line must also arise by recombination from C^{+3}, so that

$$E_r(\lambda1909) = N(C^{+3}) N_e \alpha_r h\nu , \qquad (3)$$

where α_r is the effective recombination coefficient. From Storey (1981), the dominant dielectronic recombination rate can be written approximately as

$$\alpha_r = 7.43 \times 10^{-12} t^{-0.93} . \qquad (4)$$

Combining the above three equations,

$$\frac{E_r(\lambda1909)}{E_c(\lambda1909)} = 8.20 \times 10^{-5} t^{-0.39} e^{7.54/t} \frac{N(C^{+3})}{N(C^{+2})} . \qquad (5)$$

For low-excitation nebulae, the ratio is kept small through negligible C^{+3}. As excitation and $N(C^{+3})/N(C^{+2})$ climb, so does t (see Kaler 1986), which keeps E_r/E_c low. From a variety of studies (Aller and Czyzak 1983; Barker 1982, 1983, 1984, 1985, 1986; Harrington *et al.* 1982), $N(C^{+3})$ does not approximate $N(C^{+2})$ until the He II λ4686 line strength is roughly half that of $H\beta$, by which point $t \approx 1.25$ and E_r/E_c is only 0.03. Radiative recombination should add less than a factor of 1.5 to the above ratio (Storey 1981). It is unlikely that we would find a combination of circumstances that could enhance the collisionally excited λ1909 line by more than $\sim$20%, and consequently recombination can be ignored, particularly in light of the accuracy of the observational data.

The C II λ4267 line is generally assumed to arise from radiative recombination, although some doubt, at least for extreme circumstances (namely high excitation, see for example Barker 1984), still exists. Dielectronic recombination is not important (Storey (1981). Writing from Pengelly (1963) and Brocklehurst

(1971), Torres-Piembert, Peimbert, and Daltabuit (1980a) give

$$N(\mathrm{C}^{+2})/N(\mathrm{H}^{+}) = 0.109t^{0.14}E(\lambda4267)/E(\mathrm{H}\beta) . \quad (6)$$

From

$$E(\mathrm{H}\beta) = N(\mathrm{H}^{+})N_e\alpha(\mathrm{H}\beta)h\nu , \quad (7)$$

and from a best fit to Brocklehurst's (1971) recombination coefficients that gives

$$\alpha(\mathrm{H}\beta) = 3.03 \times 10^{-14}t^{-0.89} , \quad (8)$$

we may write

$$E(\mathrm{C\ II}\ \lambda4267) = 1.136 \times 10^{-24}t^{-1.03}N(\mathrm{C}^{+2})N_e , \quad (9)$$

which, combined with equation (2), yields

$$\frac{E(\mathrm{C\ III]}\ \lambda1909)}{E(\mathrm{C\ II}\ \lambda4267)} = 8.30 \times 10^5 t^{0.49} e^{-7.5364/t} . \quad (10)$$

This ratio is equated with the observed intensity ratio, $I(\lambda1909)/I(\lambda4267)$, hereafter called R_c, and is plotted as the solid line in Figure 1.

b) *Observations*

The nebulae for which both C II λ4267 and C III] λ1909 fluxes have been determined are listed in Table 1. The major obstacle in calculating the flux ratio of these two lines is in the

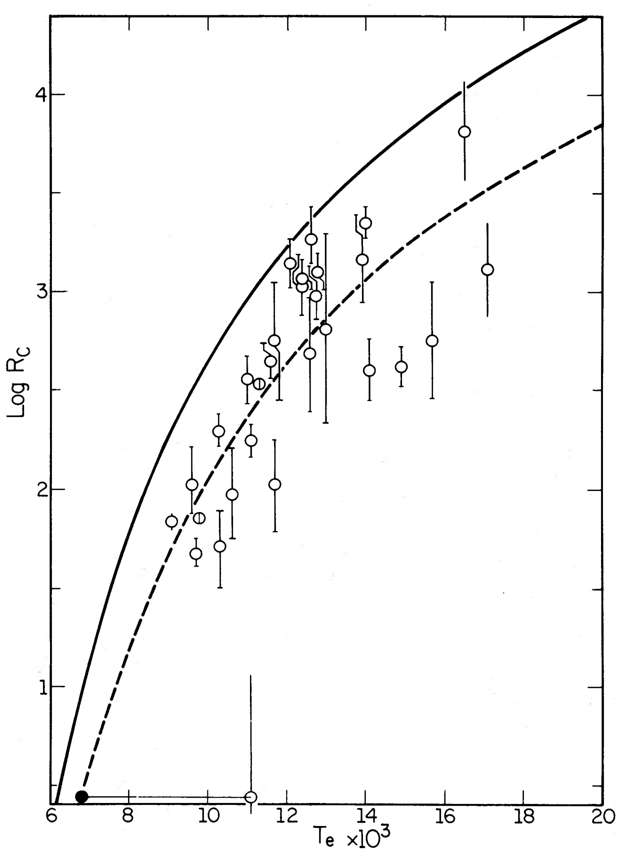

FIG. 1.—log R_c = log [I(C III] λ1909/I(C II λ4267)] vs. electron temperature. *Solid curve*: theoretical ratio from eq. (10), using existing atomic parameters; *dashed curve*: empirically corrected ratio, in which α(λ4267) would be increased by a factor of 3.76 (§ III); *open circles*: observed log R_c vs. T_e[O III]; *filled circle*: the same for M4-18 plotted with T_e[N II].

proper scaling of UV surface brightness (partial fluxes) to total optical fluxes in cases in which the nebulae are larger than the 10″ × 20″ *IUE* aperture. The C III] data to be evaluated, and if necessary corrected, are presented (in units of 10^{-12} ergs cm^{-2} s^{-1}) in column (2) of the table, with a reference code in column (4). All are taken from observations made with the *International Ultraviolet Explorer* (*IUE*). Boggess, Feibelman, and McCracken (1980) note that the line is saturated for NGC 6644; however, comparisons between other lines so designated and unsaturated observations indicate that the extrapolated flux is likely to be accurate.

There are three ways of determining the aperture correction factor A: (1) comparison of common lines in the λλ3000–3200 band observed from space and from the ground; (2) comparison of the He II λ4686 total fluxes with the He II λ1640 surface brightnesses (hereafter the λ1640/λ4686 ratio); and (3) calculation of the fractional area of the nebula accepted by the *IUE* aperture. The first of these is especially poor: the ground-based data are compromised both by uncertain atmospheric absorption corrections and because most were obtained photographically with large and unknown errors; in addition, the *IUE* observations suffer from end effects in the LWR detector.

High-quality data are available for the second method, however, for which

$$A(\mathrm{He\ II}) = \frac{E(\lambda1640)}{E(\lambda4686)} \Bigg/ \left[\frac{F(\lambda1640)}{F(\lambda4686)} \times 10^{c\Delta f}\right] , \quad (11)$$

where $E(\lambda1640)/E(\lambda4686)$ is the theoretical ratio determined from recombination theory, c is the usual logarithmic extinction at Hβ, and Δf the difference in the reddening function between the two lines. For now, we will ignore the true angular sizes of the nebulae (see col. [11] of Table 1) and calculate A(He II) for each object strictly according to the above equation (even if the value is less than unity). The references of column (4) also provide the λ1640 (total or surface) fluxes, which are given in column (3). The observed Hβ fluxes are presented in column (5). These are multiplied by the observed $I(\lambda4686)/I(\lambda4861)$ intensity ratios so as to generate the total He II λ4686 ratios of column (6). The optical data are taken from a general compilation of the literature by Cahn and Kaler (1986). The relative λ4686 strengths are preferentially from wide-aperture photometry.

The extinction constants, with one exception derived from Hα/Hβ ratios, are given in column (7). The reddening function used in a composite of those published by Whitford (1958) and Savage and Mathis (1979), for which $\Delta f = 1.105$. The observed λ1640/λ4686 flux ratios, corrected for extinction (the denominator in equation [11]), are then presented in column (8). The theoretical ratios (the numerator of equation [11]) have been calculated as functions of electron temperature and density by Seaton (1978), and are listed in column (9). The extinction constants and electron temperatures (see Table 2) and densities are taken from the compilation by Kaler (1986). Four nebulae are not considered there: data for NGC 6565, NGC 6891, and IC 4997 are from Kohoutek and Martin (1981); Kaler, Aller, and Czyzak (1976); and O'Dell (1963) respectively; and for NGC 6741 from Kaler and Lutz (1985) and Aller, Keyes, and Czyzak (1985). (The calculated parameters for NGC 6565, not listed in Table 2, are T_e = 8100 K, N_e = 300 cm^{-3}).

The helium aperture corrections, A(He II), are listed in column (10). Note that two values (for IC 1297 and NGC 6565) are less than unity, which is an expected result of observational

TABLE 1

ULTRAVIOLET DATA AND APERTURE CORRECTIONS

	$10^{12}\ S_\lambda d\lambda$ [a]			$10^{12}\ F_\lambda d\lambda$									
Nebula	C III] λ1909	He II λ1640	UV Ref	Hβ	He II λ4686	c	obs $\frac{I(\lambda1640)}{I(\lambda4686)}$	Theoret. $\frac{I(\lambda1640)}{I(\lambda4686)}$	A (He II)	ø" in	ø" out	A (ø)[b]	A
(1)	(2)	(3)	(4)	(5)	(6)	(7)	(8)	(9)	(10)	(11)		(12)	(13)
NGC 1535	8.26	14.3	BFM	35.5	5.32	0.10	3.47	6.70	1.93	9.3	23	4.34	3.14±1.21
NGC 2022	6.05	9.78	CC	7.41	6.59	0.43	4.43	7.00	1.58	10	14	2.17	1.87±0.29
NGC 2371	2.51	7.33	PGGW	10.2	9.51	0.13	1.07	6.94	6.49	27	...	10.6	8.55±2.06
NGC 2440	42	27	SAKC[c]	31.6	21.2	0.33	2.95	6.95	2.36	8	20	3.40	2.88±0.52
NGC 2867	42.1	16.3	AKRO[c]	25.7	7.20	0.40	6.26	6.72	1.08	6	...	1.08	1.08±0.0
NGC 3242	98.1	84[d]	BFM	162	43.7	0.08	2.36	6.70	2.84	11	19	3.5	3.17±0.33
NGC 6302	1.49	1.57	AROK[c]	28.2	15.8	1.13	1.76	7.36	4.18	30	...	13.1	8.64±4.46
NGC 6537	0.025	0.085	FAKC[c]	3.98	2.59	2.04	5.87	7.14	1.22	6[e]	...	1.08	1.15±0.07
NGC 6565	...	2.04	BFM	6.17	0.74	0.40	7.63	6.30	0.83	4.5	...	1.0	1.0
NGC 6572	50.5	...	CC,FP,TP	155	...	0.34	...	...	...	7.5	...	1.27s	1.27
NGC 6644	12.3	2.39	BFM	10.5	1.78	0.38	3.53	6.82	1.93	1.2	...	1.0	1.0
NGC 6741	0.81	0.40	AKC[c]	4.47	1.94	1.09	3.30	6.75	2.05	4	...	1.0	1.0
NGC 6818	35.9	21.9	BFM	34.7	17.7	0.31	2.72	6.82	2.51	11x7.5	...	1.7r	2.11±0.41
NGC 6886	1.75	0.66	APC	4.90	1.91	0.76	2.37	6.90	2.91	3	...	1.0	1.0
NGC 6891	3.12	...	BFM	22.4	...	0.34	...	...	...	7.5	...	1.27s	1.27
NGC 7009	25.7	40.9	BFM,CC,PB	159	22.2	0.07	2.20	6.56	2.98	14	...	2.84	2.91±0.07
NGC 7026	0.49	0.67	BFM	12.6	1.26	0.66	2.85	6.43	2.26	13	...	2.51	2.39±0.13
NGC 7027	10.3	4.34	BFM,PBB	75.9	31.1	1.24	3.27	6.86	2.10	7.5	...	1.5r	1.80±0.30
NGC 7662	93.0	95.6	HSAL,PT	102	50.1	0.15	2.79	6.80	2.44	8	15	2.29s	2.37±0.08
IC 418	28.5	...	BFM,HLSS	269	...	0.30	...	...	...	6.3	...	1.12s	1.12
IC 1297	...	15.0	BFM	10.7	3.75	0.33	9.25	6.70	0.72	3.5	...	1.0	1.0
IC 2149	4.94	...	BFM	28.2	...	0.25	...	...	...	6x3	7.5x5	1.1r	1.1
IC 2165	22.3	6.75	CC	12.6	5.16	0.45	4.11	6.95	1.64	4	...	1.0	1.0
IC 2448	...	20.4	TPD1	14.5	4.33	0.13	6.56	6.80	1.04	4	...	1.0	1.0
IC 4997	19.6	...	BFM,CC,F,FB	29.5	...	0.52	...	...	...	1	...	1.0	1.0
Hu1-2	3.95	5.55	BFM	6.17	5.86	0.59	4.25	7.22	1.70	2.5	...	1.0	1.0
Hu2-1	1.81	...	BFM,LU	15.9	...	0.49	...	...	...	1.5	...	1.0	1.0
J 320	7.76	1.88	BFM	4.07	0.12	0.23	28	...	...	5.5x4	...	1.05	1.05
J 900	7.92	1.65	BFM,CC	4.79	1.87	0.71	5.37	6.78	1.26	5x4	...	1.0	1.0
M4-18	0.119	...	GD[c]	1.18	...	1.0	...	...	...	< 1	...	1.0	1.0
Me2-1	16.5	14.0	AKC1[c]	4.57	3.70	0.11	5.01	6.77	1.35	4	...	1.0	1.0

[a] Parentheses enclose calculated or estimated percentage errors.
[b] These references also in Table 1.
[c] From, or averaged with, the results of Table 3.

REFERENCES.—(AKRO) Aller *et al.* 1981*b*. (AKC) Aller *et al.* 1985. (AKC1) Aller *et al.* 1981*a*. (APC) Aller 1985. (AROK) Aller *et al.* 1981*c*. (BFM) Boggess *et al.* 1980. (CC) Carpenter and Czyzak 1982. (F) Flower 1980. (FAKC) Feibelman *et al.* 1985. (FB) Feibelman 1982. (FP) Flower and Penn 1981. (GD) Goodrich and Dahari 1985. (HLSS) Harrington *et al.* 1980. (HSAL) Harrington *et al.* 1982. (LU) Lutz 1981. (PB) Perinotto and Benvenuti 1981. (PBB) Perinotto *et al.* 1980. (PGGW) Pottasch *et al.* 1981. (PT) Peña and Torres-Peimbert 1981. (SAKC) Shields *et al.* 1981. (TP) Torres-Peimbert and Peña 1981. (TPD1) Torres-Peimbert *et al.* 1980*b*.

TABLE 2

LINE RATIOS AND TEMPERATURE ANALYSIS

Nebula	I(Hβ) = 100[a]: I(C III] λ1909)	I(C II λ4267)	Ref	log R_c	T_e (C^{2+})	T_e [O III]	T_e [N II]	log T_* / Ex	log R_c^O	log R_c^N	T_e' (C^{2+})
(1)	(2)	(3)	(4)	(5)	(6)	(7)	(8)	(9)	(10)	(11)	(12)
NGC 1535	95.9 (67)	0.90 (20)	AC1,GMC,K	2.03±0.23	8500± 500	11700	(11300)	15	3.15	(3.05)	9900
NGC 2022	492 (19)	1.15 (20)	AC2,K	2.63±0.10	10000± 300	14900	(10100)	93	3.81	(2.68)	11900
NGC 2371	298 (35)	0.73 (21)	AC2,K	2.61±0.15	9900± 500	14100	9600	94	3.67	2.50	11900
NGC 2440	939 (20)	0.41 (2)	SAKC[b],K	3.36±0.08	12500± 400	14000	10100	69	3.65	2.68	15800
NGC 2867	525 (10)	1.17 (21)	AKRO[b],GMC	2.65±0.09	10000± 300	11600	9800	30	3.13	2.57	12000
NGC 3242	239 (11)	0.73 (2)	AC1,K	2.54±0.02[c]	9700± 100	11300	10100	27	3.05	2.68	11600
NGC 6302	985 (80)	0.15	AROK[b]	3.82±0.26	15000±1700	16500	16400	63	4.04	4.03	19700
NGC 6537	185 (100:)	0.32	FAKC[b]	2.76±0.30	10400±1000	15700	16800	80	3.93	4.08	12500
NGC 6572	104 (10)	0.52 (19)	AC1,FR,K	2.30±0.08	9100± 200	10300	(10500)	4.78	2.75	(2.81)	10700
NGC 6644	330 (93)	0.68 (18)	K,W	2.69±0.29	10200± 900	12600	13600	18	3.37	3.58	12200
NGC 6720	...	...	...	2.25±0.08[c]	9000± 200	11100	10600	28	2.99	2.84	10600
NGC 6741	350 (100)	0.62 (13)	AKC[b],K	2.75±0.30	10300±1000	11700	9400	48	3.15	2.42	12400
NGC 6818	509 (22)	0.40 (10)	AC1,FR	3.10±0.09	11500± 400	12800	11400	53	3.41	3.08	14200
NGC 6853	...	...	...	2.56±0.12[c]	9800± 300	11000	10000	33	2.96	2.65	11700
NGC 6886	282 (200)	0.44	AC1	2.81±0.48	10500±1800	13000	10600	42	3.46	2.84	12700
NGC 6891	45 (50)	0.48 (44)	FR,K	1.97±0.22	8400± 600	10600	(11800)	4.69	2.83	(3.17)	9800
NGC 7009	57.1 (10)	0.77 (8)	CA,FR,K	1.86±0.01[c]	8200± 100	9800	11000	14	2.57	2.96	9500
NGC 7026	55.9 (10)	0.81 (7)	AC1,FR,K	1.84±0.05	8100± 100	9100	9500	11	2.30	2.46	9400
NGC 7027	709 (18)	0.60 (13)	FR,KACE	3.07±0.09	11400± 300	12400	(10300)	47	3.32	(2.75)	14000
NGC 7662	326 (10)	0.54 (10)	AC2,FR,K	3.00±0.18[c]	11200± 700	12800	10600	48	3.42	2.83	13600
IC 418	26.7 (10)	0.56 (15)	AC2,K,FR,TPD	1.68±0.07	7800± 200	9700	(8200)	4.51	2.54	(1.88)	9000
IC 2149	38.1 (45)	0.73 (20:)	TPP	1.72±0.17	7900± 300	10300	8700	4.56	2.75	2.13	9100
IC 2165	602 (64)	0.41 (12)	AC1,GMC,K	3.17±0.22	11800± 900	13900	9700	43	3.63	2.54	14600
IC 4997	273 (10)	0.19 (50:)		3.16±0.18	11700± 600	...	...	4.69	...	...	14500
Hu1-2	318 (70)	0.24 (27)	AC2,K	3.12±0.24	11600± 900	17100	11600	101	4.12	3.13	14300
Hu2-1	43.2 (55)	0.40 (13)	AC2,FR	2.03±0.19	8500± 500	9600	13300	4.56	2.50	3.52	9900
J 320	374 (40)	0.20 (20:)	AC2	3.27±0.16	12200± 400	12600	13600	4.76	3.37	3.58	15200
J 900	1138 (26)	0.81 (20:)	AC2	3.15±0.12	11700± 500	12100	10600	42	3.25	2.84	14400
M4-18	153 (100:)	35.3 (10:)	GD[b]	0.64±0.43	6400± 500	(11100)	6800	4.34	(2.99)	1.02	7000
Me2-1	487 (35)	0.44 (20:)	AKC1[b]	3.04±0.15	11300± 300	12400	11600	82	3.32	3.13	13900

[a] As observed through *IUE* aperture.
[b] s, segment of circle excluded by aperture; r, nebula assumed to be rectangle.
[c] Reference source for C II λ4267; see Table 2.
[d] Determined from He II λλ3203, 2734.
[e] Inner core; faint outer region ignored.

REFERENCES (in alphabetical order).—(AC1) Aller and Czyzak 1979. (AC2) Aller and Czyzak 1983. (AKC) Aller *et al.* 1981*a*. (AKRO) Aller *et al.* 1981*b*. (AROK) Aller *et al.* 1981*c*. (CA) Czyzak and Aller 1979. (FAKC) Feibelman *et al.* 1985. (FR) French 1981. (GD) Goodrich and Dahari 1985. (GMC) Gutiérrez-Moreno *et al.* 1985. (K) Kaler 1981, (KACE) Kaler *et al.* 1976. (SAKC) Shields *et al.* 1981. (TPD) Torres-Peimbert *et al.* 1980*a*. (TPP) Torres-Peimbert and Peimbert 1977. (W) Webster 1984.

error; also, the observed $\lambda1640/\lambda4686$ ratio for J320 is totally unrealistic and is subsequently ignored. Finally, He II $\lambda1640$ is not listed for NGC 3242 in Boggess, Feibelman, and McCracken's (1980) catalog as it was saturated, and A(He II) is based on He II $\lambda3203$, $\lambda2734$, and Seaton's (1978) theoretical ratios.

There are serious problems with the use of the He II lines in the derivation of the aperture correction. First, of course, the method is unavailable for the lower excitation objects. The second stems from nebular stratification, in that the optical and UV data are not measured in the same positions. For example, if the *IUE* aperture is centered in a large nebula, where the He^{+2} ions are concentrated, and the $\lambda4686$ strength is derived from wide-aperture photometry, A(He II) will be underestimated, possibly by a factor of 2 or more. Other aperture settings could as easily yield an overestimate.

Method (3) above is more direct, but certainly not without peril. The problem here is the considerable irregularity of the emitting surface. Without the aperture settings and isophotic contours of the C III] line, which are unavailable, errors are inevitable. By default, we may simply assume that the nebulae larger than the aperture are uniformly illuminated. The angular area of the aperture is 219 arsec^2 from Bohlin *et al.* (1980), for an effective circular radius r of 8".3. The angular radii are taken from Perek and Kohoutek (1967) and are listed in column (11) of Table 1. Four nebulae have distinct outer shells, for which both the inner and outer radii are given.

For nebulae that fill the aperture, the listed radii are harmonic means of the major and minor axes, and $A(\phi) = \phi^2/r^2$, given in column (12). For nebulae with outer shells, the adopted aperture correction is the mean of $A(\phi_{in})$ and $A(\phi_{out})$, which weights the correction toward the brighter, inner ring. The correction, of course, is just unity for nebulae completely contained within the aperture. A few objects fit within one axis of the oval *IUE* aperture but spill out the other. For most, the equivalent circular nebula was positioned over the aperture, and the approximate correction determined by the size of the excluded segments ("s" in col. [12]). Others were considered rectangles ("r"), and the adopted $A(\phi)$ is the mean of those found by positioning the object along and perpendicular to the major axis.

For the larger objects, the agreement between A(He II) and $A(\phi)$ is quite reasonable: the average deviation from the mean is $\sim 15\%$. The agreement is worst for the largest nebula, NGC 6302, but even there, the mean correction should be within a factor of 2 of being correct. The smaller nebulae, those for which $A(\phi) = 1$ (including NGC 2867, since its value is so close), present a conundrum: in most cases, the A(He II) are greater than unity, some considerably so. To help examine this problem, three additional small nebulae for which both carbon lines have not been measured (all those available: NGC 6565, IC 1297, and IC 2448) are included in Table 1. For these 11 small objects, $\bar{A}$(He II) $= 1.49 \pm 0.19$. It is very unlikely that there could be an error in theory, or in the optical He II data. The problem might be in the correction for interstellar reddening. If the extinction constants derived from radio fluxes are substituted in column (7), the discrepancy is considerably diminished, as these average larger than those computed from $H\alpha/H\beta$ ratios (see Kaler and Lutz 1985; Gutiérrez-Moreno, Moreno, and Cortés 1985). And the average correction for these small nebulae can, within the observational error, be brought to unity if the radio extinctions are combined with the reddening function of Code *et al.* (1976). However, the problem could as easily be a result of the small number of objects examined, combined with random and systematic error. Inspection of Table 1 shows that A(He II) correlates negatively with $F(\lambda1640)$: especially, the two largest values of A(He II) are associated with by far the weakest fluxes. Consequently, the discrepancies may simply rest on systematic error that depends on signal strength. If we use only the four nebulae with $F(\lambda1640) > 10^{-11}$, $\bar{A}$(He II) $= 1.03 \pm 0.13$, as would be expected.

Finally, the adopted corrections A are shown in column (13). For nebulae for which $A(\phi) = 1$, $A = 1$, no matter what the value of A(He II). Otherwise, A is a mean of the two. If A(He II) < 1, it is first set equal to unity. For the larger nebulae that require correction factors, the error (simply defined as $|A - A(\phi)|$) is given.

We are now able to calculate the corrected fluxes of the C III] $\lambda1909$ lines relative to Hβ, or $I(\lambda1909)$ as placed on the usual scale $I(H\beta) = 100$,

$$I(\lambda1909) = 100\,\frac{S(\lambda1909)}{F(H\beta)}\,A \times 10^{cf(\lambda1909)}\,, \qquad (12)$$

where $f(\lambda1909) = 1.18$. These are given in column (2) of Table 2. The numbers in parentheses following the values are estimated percentage errors derived from the data of Table 1. We would expect the errors assigned to the observed flux of C III] $\lambda1909$ and consequently to $I(\lambda1909)$ in equation (12), to be similar to that for $S(\lambda1640)$, so that we can make use of those given in column (13) of Table 1. However, not all nebulae have He II lines; for these, no error estimate is available, so that we must resort to indirect means. These errors are assessed by plotting the percentage errors attached to A in Table 1 against $S(\lambda1640)$. For the nebulae with measured A(He II) for which $A(\phi) = 1$, the percentage error is taken to be 100 $|A(\text{He II}) - A(\phi)|$. A mean line is then drawn through all the points and the curve now applied to $S(\lambda1909)$. The error in column (13) of Table 1 is attached to $S(\lambda1909)$ if that flux is greater than $S(\lambda1640)$ and is scaled upward according to the curve if $S(\lambda1909)$ is less than $S(\lambda1640)$. If A(He II) is not available, the curve is applied directly, substituting $S(\lambda1909)$ in the abscissa. In no case is the error allowed to fall below the mean error at high flux levels, which is $\pm 10\%$. The errors for NGC 6537 and M4-18 are arbitrarily placed at $\pm 100\%$ because of the weakness of the lines. Errors in the extinction constants also affect $I(\lambda1909)$. However, they are generally small; in any case, $\lambda1909$ and $\lambda1640$ will be affected similarly, so that the extinction errors will be compensated for by A(He II) and will then largely be included in the errors in Table 1. The exceptions are the nebulae with no A(He II) and with larger extinction errors (NGC 6891, ± 0.05; J320, ± 0.06; M4-18, ± 0.3), for which the effect is added quadratically to the errors described above.

The next step is the presentation of C II ($\lambda4267$) intensities in column (3), taken from the references of column (4). Those from Kaler (1981) are the corrected older photographic values, further corrected for changes in the extinction coefficients used here (applied to $f_\lambda = 0.15$). All photoelectrically determined values are referenced. Two measurements are available for just over half the nebulae, and again the numbers in parentheses are the percentage errors derived from comparing the individual values. A generic 10% or 20% error is assigned to single measurements, based purely on subjective judgement. For the few $\lambda4267$ intensities without errors, those attached to $I(\lambda1909)$ are so large that the $\lambda4267$ error is not likely to be very relevant.

Finally, the log of the ratio $I(\lambda 1909)/I(\lambda 4267) = R_c$ is presented in column (5) of Table 2, in which the errors are quadratically compounded from those in columns (2) and (3). Five nebulae, indicated by footnote *c*, are treated somewhat differently. These have been observed by Barker (1982, 1983, 1984, 1985, 1986). The values of log R_c for the various positions (col. [2] of Table 3) observed in these objects are given in column (2) of Table 3, corrected for the slightly different extinction functions and constants used here. The means of Barker's observations are given at the end of the listing of each nebula. These means are averaged with R_c derived from columns (2) and (3) of Table 2, with the result presented in column (5) of Table 2, where the error indicates the difference between the two. For NGC 7662 the extinctions specific to Barker's (1986) regions were calculated from his Hα/Hβ ratios. His mean log R_c is 0.44 above the mean calculated from the other references, supporting his feeling that his *IUE* aperture correction could be overestimated by a factor of 2 or more. (The error in the log in Table 2 is the average of the individual plus and minus departures). However, given the general difficulty with these corrections, it is probably best to treat this nebula like any other and average all the data. Finally, note here that the errors presented in Table 2 can only be approximate. They are not derived by any standard method of analysis and are meant only as a coarse guide to the reader and to subsequent analysis.

TABLE 3

POINT-BY-POINT OBSERVATIONS

Region (1)	log R_c (2)	$T_e(C^{+2})$ (3)	T_e[O II] (4)	T_e[N II] (5)	$T'_e(C^{+2})$ (6)
NGC 3242 (Barker 1985); $c = 0.08$					
1	2.35	9300	11500	...	10900
2	2.57	9800	11100	...	11700
3	2.47	9500	11200	...	11300
4	2.67	10100	11200	...	12100
5	2.73	10300	10600	...	12400
Mean	2.56 ± 0.06	9800	11100	...	11700
NGC 6720 (Barker 1982); $c = 0.29$					
1E	2.10	8600	11500	13800	10100
3E	2.36	9300	10300	13200	10900
4E	2.29	9100	9300	9200	10700
Mean	2.25 ± 0.08	9000	10400	12100	10600
NGC 6853 (Barker 1984); $c = 0.18$					
2	2.55	9800	11300	10100	11600
3	2.86	10700	10900	9600	13000
4	2.54	9700	9900	9600	11600
7	2.27	9000	8900	10600	10600
Mean	2.56 ± 0.12	9800	10300	10000	11700
NGC 7009 (Barker 1983); $c = 0.07$					
1	1.80	8000	10300	...	9300
2	1.90	8200	9400	...	9600
3	1.75	7900	9800	...	9200
4	1.95	8300	9200	9700	9700
Mean	1.85 ± 0.05	8100	9700	9700	9500
NGC 7662 (Barker 1986); c varies[a]					
1	3.06	11400	13900	...	13900
2	3.17	11800	13300	...	14600
3	3.14	11700	12400	...	14400
4	3.13[b]	11600	11700	...	14300
5	3.22[b]	12000	11400	11400	14900
Mean	3.15 ± 0.03				

[a] c = 0.25, 0.16, 0.34, 0.36, 0.35 for regions 1–5.

[b] Corrected by aperture area $A(\phi)$ instead of by the He II lines.

III. TEMPERATURE ANALYSIS

We can now enter the curve of Figure 1 with the values of log R_c to determine the electron temperatures of the C^{+2} zones, $T_e(C^{+2})$, shown in column (6) of Table 2. For comparison, the mean [O III] and [N II] temperatures from Kaler (1986) are shown in columns (7) and (8); estimated values derived from the correlations between temperature and excitation put forward in that study are set in parentheses. For the nebulae not included therein, see the references cited in § II*b*. The values for IC 4997 are not given because of their uncertainty. The same data are presented for the specific regions of the five nebulae in Table 3 (see § IV). For further analysis, the excitation levels of the nebulae are given in column (9) of Table 2, as expressed by I(He II λ4686) or central star temperature (T_*), also from Kaler (1986) or from references therein.

The data are plotted in several ways in Figures 1–7 to illustrate the thesis of this paper, that $T_e(C^{+2})$ is similar to T_e[O III], except at very low excitation levels or central star temperatures, and that an adjustment must be made to some atomic parameter, most likely the effective recombination coefficient of C II λ4267. Figure 2 shows $T_e(C^{+2})$ versus T_e[O III]. Note that the two correlate quite well, except for an offshift, with $T_e(C^{+2})$ averaging about 2000 K lower than the other. The triangle is based on an estimate of T_e[O III] for the very low excitation object M4-18 and fits poorly. Figure 3 shows $T_e(C^{+2})$ plotted against T_e[N II]. Now the mean fit is improved, with $T_e(C^{+2})$ averaging roughly 1000 K lower, but the actual correlation is clearly worse.

These two comparisons are further elucidated by plotting $T_e(C^{+2})$ against the combination of log T_* and $I(\lambda 4686)$ [called log T_*–$I(\lambda 4686)$] in Figure 4, where the curves are the median distributions for T_e[O III] and T_e[N II] from Kaler (1986). Again, but for a fairly constant offshift, the C^{+2} points seem to follow the [O III] line better than the [N II] curve, with the exception of the far left-hand point that represents M4-18, indicates a low temperature, and qualitatively fits the [N II] line. (The filled symbol represents IC 4997, which has an unusually high density, and which is discussed in § IV). Figure 4 reflects a steep climb in log R_c with excitation that appears with the onset of He II λ4686. This correlation could be mistakenly interpreted as a weakening of I(C II λ4267) caused by a change in the excitation mechanism of the line (e.g., fluorescence changing over to recombination), where it not for the clear fact that this behavior might be expected due to the increase of [O III] temperature with I(He II λ4686).

Another illustration is given by examining the differences between the observed log R_c and those expected from Figure 1 calculated on the basis of T_e[O III] and T_e[N II]. The predicted ratios, called R_c^{O} and R_c^{N} respectively, are given in columns (10) and (11) of Table 2; parentheses again indicate estimates. The differences log R_c^{O} − log $R_c = \Delta^{\mathrm{O}}$ and log R_c^{N} − log $R_c = \Delta^{\mathrm{N}}$ are shown in Figure 5 by open and filled symbols respectively; values from estimated [O III] or [N II] temperatures are indicated by smaller symbols. We see that Δ^{O} exhibits a slow decline as excitation increases, especially for O $\lesssim I(\lambda 4686) \lesssim$ 80, beyond which point it again shows high values. Nevertheless, Δ^{O} presents a considerably flatter correlation with $I(\lambda 4686)$ than Δ^{N}, which drops quite sharply. M4-18 represents a distinct case, for which Δ^{N} clearly fits into the diagram better than Δ^{O}.

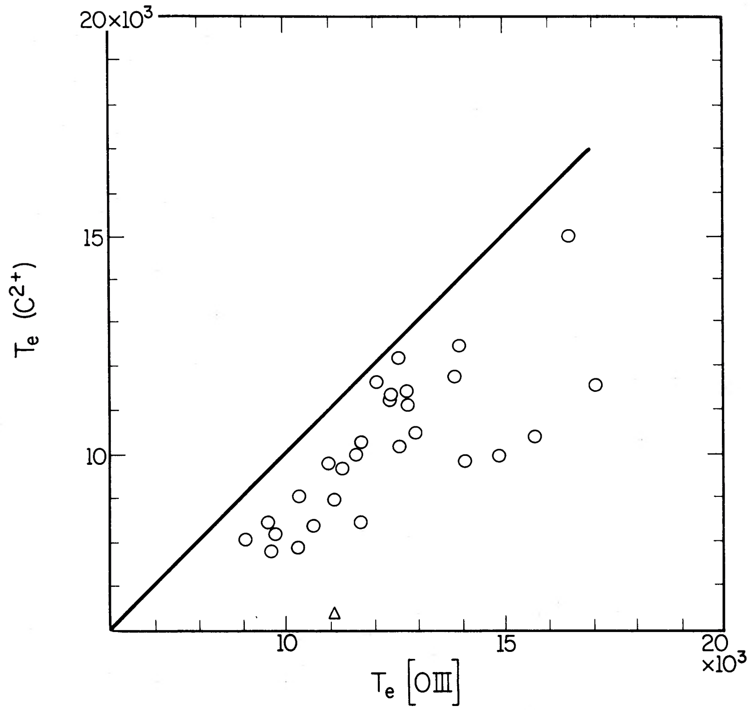

FIG. 2.—$T_e(C^{+2})$ from the observations and the solid curve of Fig. 1 vs. T_e[O III]. The triangle represents M4-18, for which T_e[O III] is estimated from T_e[N II] and Kaler's (1986) relation.

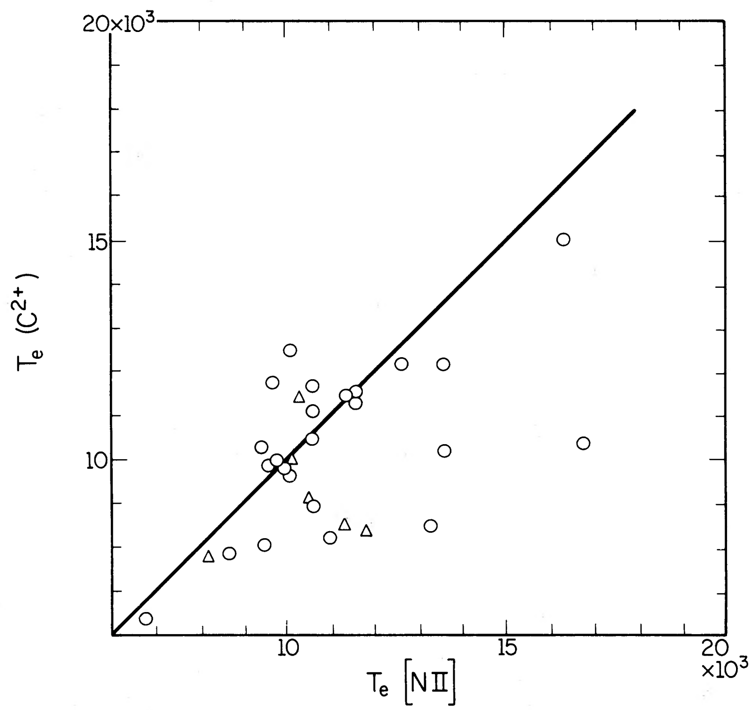

FIG. 3.—$T_e(C^{+2})$ from the observations and the solid curve of Fig. 1 vs. T_e[N II]. *Triangles*, nebulae for which T_e[N II] is estimated from T_e[O III] and Kaler's (1986) relation.

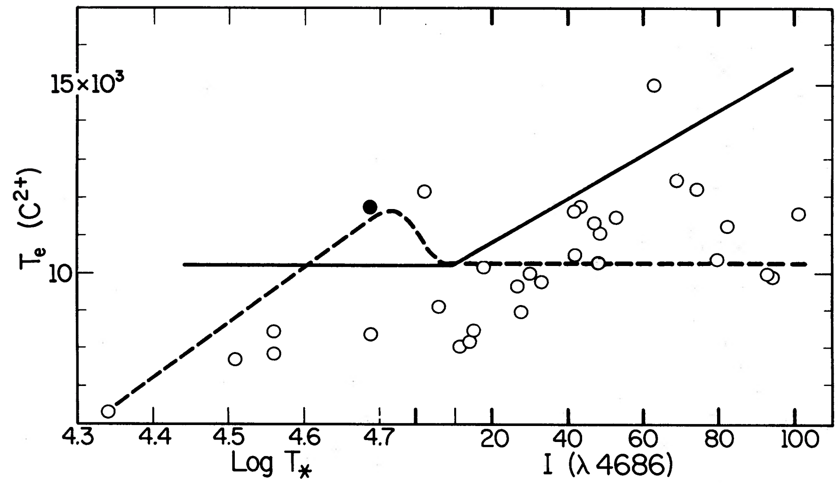

FIG. 4.—$T_e(C^{+2})$ from the solid curve of Fig. 1 vs. log T_* or $I(\lambda4686)$, where $I(\lambda4686) = 0$ for log $T_* = 4.75$. *Filled circle*, IC 4997, which is ignored in the analysis because of its unusual nature. The solid and dashed line respectively show the median values of T_e[O III] and T_e[N II] from Kaler (1986).

From the better correlative agreement between $T_e(C^{+2})$ and T_e[O III], let us assume for the present that the two should, on the average, be the same and that the general offshift seen in the figure is caused simply by miscalculation of an atomic parameter that enters into $R_c(T_e)$. Under this assumption, the observed log R_c are plotted against T_e[O III] in Figure 1, the one exception being M4-18, which is plotted against T_e[N II] as well, which we again see fits better. Clearly, a superior fit will be attained by lowering the theoretical curve.

An empirical correction to $R_c(T_e)$ (eq. [10]) can now easily be effected by determining the mean R_c^O/R_c. However, we must be cautious. The ionization potentials of C^{+2} are between those of N^+ and O^{+2}, and consequently, given a smooth temperature gradient, we might expect that $T_e(C^{+2})$ could be between T_e[O III] and T_e[N II]. Since T_e[N II] is generally lower than T_e[O III], we could have a real situation in which $T_e(C^{+2})$ followed T_e[O III] but was offset below it, as seen in the figures. Consequently, let us calculate an empirical correction only from those nebulae within a restricted excitation range for which the mean T_e[N II]/T_e[O III] $= r$ is roughly unity, which from Kaler's (1986) curve is log $T_* < 4.55$, $I(\lambda4686) \leq 30$. Within these limits, r swings from 0.90 to 1.11 at log $T_* = 4.70$, and back again to 0.90. Thus the temperature gradients average out reasonably well, and the mean $T_e(C^{+2})$ should be close to the mean T_e[O III]. From Table 2, $\langle R_c^O/R_c \rangle$ for nebulae within these limits is 5.6 ± 1.1. Some of the ratios possess large errors, however. The best correction is likely found by using the best measurements, and if we now restrict

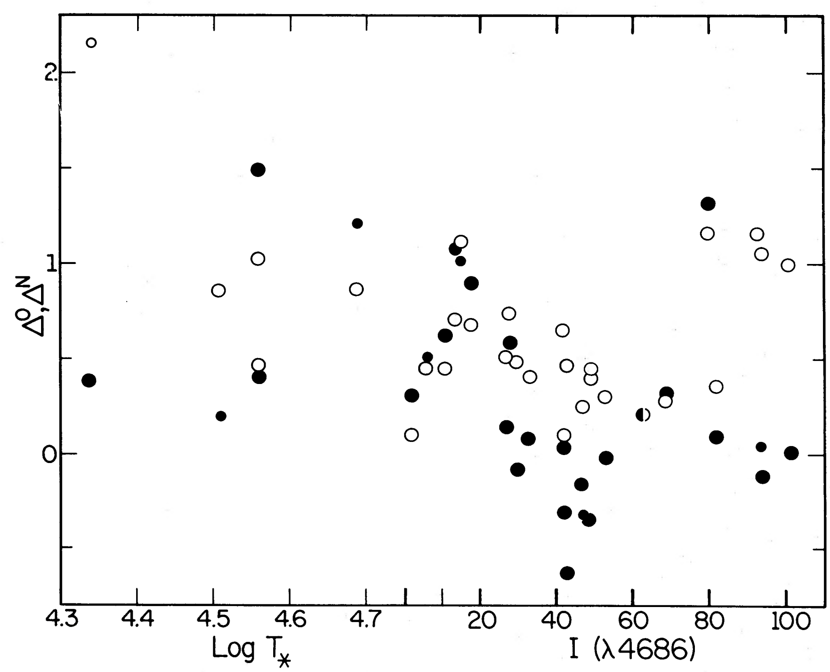

FIG. 5.—The differences between observed and predicted log R_c for T_e[O III] and T_e[N II], Δ^O and Δ^N respectively, vs. log T_* or $I(\lambda4686)$. The small symbols represent nebulae for which estimates of T_e[N II] or T_e[O III] (only M4-18) had to be made.

the data to ratios with errors or 0.10 or less in log R_c, we find $\langle R_c^O/R_c \rangle = 3.76 \pm 0.50$. (If we use all the points in the table, the mean ratio is 5.3 ± 0.8, which reflects the four high values at $I(\lambda 4686) \geq 80$; more about these later).

The next step is to divide the right-hand side of equation (10) by 3.76; the resulting curve is plotted as the dashed line in Figure 1, which we now see represents the plotted points much better. New, corrected electron temperatures, based on the empirically corrected curve of Figure 1, are presented in column (12) of Table 2, where they are called $T_e'(C^{+2})$. Figure 6 then repeats Figure 4, except that now $T_e'(C^{+2})$ is plotted against log T_*–$I(\lambda 4686)$. The fit with the T_e[O III] function is now fairly good, with M4-18 being a notable exception, and it seems to belong much more to the T_e[N II] function.

IV. DISCUSSION

Three points of discussion remain. First, assuming the argument of the previous section to be correct, which atomic parameter requires correction? From § II it has to be either the collision strength of C III] λ1909 or the effective recombination coefficient of C II λ4267. Given the complexity of the recombination process, and in the absence of other arguments, it is more likely that the widely used value for $\alpha(\lambda 4267)$ is underestimated by, crudely, a factor of 4. That means that the C^{+2}/H^+ abundances previously calculated from optical data are too high by that factor, which helps to reconcile the ultraviolet-optical discrepancy discussed in § I. It will be most interesting to see whether future detailed calculations of the recombination matrix support this contention.

Second is the matter of departures from the mean [O III] temperature function. Barker (1982, 1983, 1984, 1985, 1986) shows that the above abundance discrepancy becomes worse as we progressively consider high-excitation extremes in the nebulae. In this series of papers, he suggests that the problem lies with the excitation mechanism of C II λ4267. This idea is bolstered by the distribution of points in Figure 5, in which Δ^O is displaced upward for four high-excitation points, implying that the observed C II λ4267 line is too strong for T_e[O III]. These effects can also be described in terms of nebular temperature gradients. In Table 3, $T_e'(C^{+2})/T_e$[O III] decreases toward the nebular center. The phenomenon is seen in Figure 6, in which $T_e'(C^{+2})$ is systematically above the mean [O III] temperature for low-to-intermediate He II strengths [i.e., for $I(\lambda 4686)$ between 20 and 60] and below it for high He II strengths. It is still not clear as to whether the origin of the problem involves the excitation mechanism of C II λ4267, or whether the characteristics of the temperature gradients change as the excitation becomes very high. Can detailed models reproduce these temperature variations?

The carbon temperatures of the lower excitation nebulae, those with $4.5 < \log T_* < 4.7$, are systematically below the measured [O III] temperatures by an average of 600 K and below the median [O III] temperature for this general group (10,200 K from Kaler 1986) by about 800 K. This departure might be caused by temperature gradients and a crossover from agreement with [O III] temperatures to [N II] temperatures. There are insufficient data, however, to tell just where this crossover (anchored by M4-18) should occur.

Finally, let us consider the "forgotten nebula," IC 4997, which is listed in the tables but has so far been ignored. The problem is that the [O III] and [N II] temperatures are very uncertain because of: (1) high and unknown density (the λ3726–λ3729 doublet ratio is at the limit); and (2) the [O III] λ4363 line (and probably the [N II] λ5754 line as well) is variable (Liller and Aller 1957; Feibelman *et al.* 1979). Since R_c is not sensitive to density, we can find N_e from the [O III] electron temperature equation (Kaler 1986), $T_e'(C^{+2})$, and the appropriate [O III] line intensities. From Kaler's (1978) λ4959/Hβ ratio and Purgathofer and Stoll's (1981) mean λ4363/Hγ ratio, both of which are temporally appropriate to the *IUE* measurements, $N_e = 8.6 \pm 1.9 \times 10^5$ cm^{-3} for $T_e'(C^{+2}) = 14{,}600 \pm 1100$ K, where the error is only an estimate based on the weakness of λ4267. From Flower, Nussbaumer, and Schild (1979) and Carpenter and Czyzak (1982), $I(\lambda 1909)$/

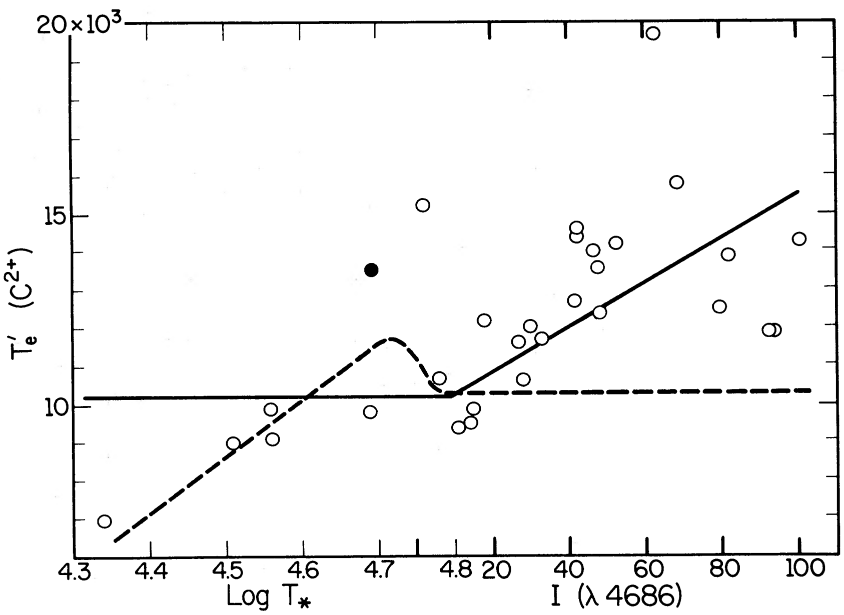

FIG. 6.—$T_e'(C^{+2})$, the corrected temperatures made on the basis of the empirically corrected function (*dashed line*) of Fig. 1, vs. log T_* or $I(\lambda 4686)$. The solid and dashed curves again respectively represent T_e[O III] and T_e[N II]. The filled symbol again represents IC 4997.

$I(\lambda 1907) = 16.4$, which from the above temperatures and Aller's (1984) theoretical curves yields $N_e = 1.0 \times 10^6$ cm^{-3}, in good agreement with the above.

In conclusion, the data indicate that the effective recombination coefficient for C II λ4267 has been rather severly underestimated, which is in part responsible for the high C/O ratios determined from optical data. Other interpretations are certainly possible: the offset between $T_e(C^{+2})$ and T_e[O III] might be caused by a combination of errors in $\gamma(\lambda 1909)$ and in $\alpha(\lambda 4267)$, and part of it may even be real, considering the very real gradients known to exist in nebulae. If the first interpretation is correct, the best abundance results from the ultraviolet C III] line would be found, of course, by using the corrected $T_e'(C^{+2})$ temperature, and in lieu of that, by using T_e[O III] for all but the lowest excitation nebulae, for which T_e[N II] might be preferable. One might also consider the residual departures in Figure 6, such as subtracting 600 K from T_e[O III] in the region $4.5 < \log T_* < 4.7$, and adding 1000 K for $40 < I(\lambda 4686) < 70$, although the paucity of data might make these corrections questionable. The highest excitation objects should probably be ignored until the Barker discrepancy can be resolved. In any case, the reader should bear in mind that the details and quantitative results of this discussion are based on small-number statistics. The conclusions presented here merely try to present the overall qualitative picture and point the way for future investigations.

This work was supported by the National Science Foundation through grants AST 80-23233 and AST 84-19355 to the University of Illinois. I would like to thank Drs. L. H. Aller and T. Barker for sending data in advance of publication, and T. Barker, W. A. Feibelman, and R. A. Shaw for comments on the manuscript.

REFERENCES

Aller, L. H. 1984, *Physics of Thermal Gaseous Nebulae* (Dordrecht: Reidel), p. 137.
———. 1985, private communication.
Aller, L. H., and Czyzak, S. J. 1979, *Ap. Space Sci.*, **62**, 397.
———. 1983, *Ap. J. Suppl.*, **51**, 211.
Aller, L. H., Keyes, C. D., and Czyzak, S. J. 1981*a*, *Ap. J.*, **250**, 596.
———. 1985, *Ap. J.*, **296**, 492.
Aller, L. H., Keyes, C. D., Ross, J. E., and O'Mara, B. J. 1981*b*, *M.N.R.A.S.*, **197**, 647.
Aller, L. H., Ross, J. E., O'Mara, B. J., and Keyes, C. D. 1981*c*, *M.N.R.A.S.*, **197**, 95.
Barker, T. 1982, *Ap. J.*, **253**, 167.
———. 1983, *Ap. J.*, **267**, 630.
———. 1984, *Ap. J.*, **284**, 589.
———. 1985, *Ap. J.*, **294**, 193.
———. 1986, *Ap. J.*, **308**, 314.
Boggess, A., Feibelman, W. A., and McCracken, C. W. 1980, in *The Universe at Ultraviolet Wavelengths: The First Two Years of IUE*, ed. R. D. Chapman (NASA Conf. Pub. No. 2171), p. 663.
Bohlin, R. C., Holm, A. V., Savage, B. D., Snijders, M. A. J., and Sparks, W. 1980, *Astr. Ap.*, **85**, 1.
Brocklehurst, M. 1971, *M.N.R.A.S.*, **153**, 471.
Cahn, J. H., and Kaler, D. B. 1986, in preparation.
Carpenter, K. G., and Czyzak, S. J. 1982, *Ap. Space Sci.* **84**, 495.
Code, A. D., Davis, J., Bless, R. C., and Brown, R. H. 1976, *Ap. J.*, **203**, 417.
Cyzak, S. J., and Aller, L. H. 1979, *M.N.R.A.S.*, **188**, 229.
Feibelman, W., 1982, *Ap. J.*, **258**, 562.
Feibelman, W. A., Aller, L. H., Keyes, C. D., and Czyzak, S. J. 1985, *Proc. Nat. Acad. Sci.*, **82**, 2202.
Feibelman, W. A., Hobbs, R. W., McCracken, C. W., and Brown, L. W. 1979, *Ap. J.*, **231**, 111.
Flower, D. R. 1980, *M.N.R.A.S.*, **193**, 511.
Flower, D. R., and Launay, J. M. 1973, *Astr. Ap.*, **29**, 321.
Flower, D. R., Nussbaumer, H., and Schild, H. 1979, *Astr. Ap.*, **72**, 21.
Flower, D. R., and Penn, C. J. 1981, *M.N.R.A.S.*, **194**, 13p.
French, H. B. 1981, *Ap. J.*, **273**, 214.
Goodrich, R. W., and Dahari, O. 1985, *Ap. J.*, **289**, 342.
Gutiérrez-Moreno, A., Moreno, H., and Cortés, G. 1985, *Pub. A.S.P.*, **97**, 397.
Harrington, J. P., Lutz, J. H., Seaton, M. J., and Stickland, D. J. 1980, *M.N.R.A.S.*, **191**, 13.
Harrington, J. P., Seaton, M. J., Adams, S., and Lutz, J. H. 1982, *M.N.R.A.S.*, **199**, 512.
Kaler, J. B. 1978, *Ap. J.*, **226**, 947.
———. 1981, *Ap. J.*, **249**, 202.
———. 1985, *Ann. Rev. Astr. Ap.*, **23**, 89.
———. 1986. 1986, *Ap. J.*, **308**, 322.
Kaler, J. B., Aller, L. H., and Czyzak, S. J. 1976, *Ap. J.*, **203**, 636.
Kaler, J. B., Aller, L. H., Czyzak, S. J., and Epps, H. W. 1976, *Ap. J. Suppl.*, **31**, 163.
Kaler, J. B., and Lutz. J. H. 1985, *Pub. A.S.P.*, **97**, 700.
Kohoutek, L., and Martin, W. 1981, *Astr. Ap. Suppl.*, **44**, 325.
Liller, W., and Aller, L. H. 1957, *Sky and Tel.*, **16**, 222.
Lutz, J. H. 1981, *Ap. J.*, **247**, 144.
Nussbaumer, H., and Storey, P. J. 1978, *Astr. Ap.*, **64**, 139.
O'Dell, C. R. 1963, *Ap. J.*, **138**, 1018.
Peña, M., and Torres-Peimbert, S. 1981, *Rev. Mexicana Astr. Ap.*, **6**, 309.
Pengelly, R. M. 1963, Ph.D. thesis, University of London.
Perek, L., and Kohoutek, L. 1967, *Catalogue of Galactic Planetary Nebulae* (Prague: Czchoslovakia Academy of Science).
Perinotto, M., and Benvenuti, P. 1981, *Astr. Ap.*, **101**, 88.
Perinotto, M., Panagia, N., and Benvenuti, P. 1980, *Astr. Ap.*, **85**, 332.
Pottasch, S. R., Gathier, R., Gilra, D. P., and Wesselius, P. R. 1981, *Astr. Ap.*, **102**, 237.
Purgathofer, A., and Stoll, M. 1981, *Astr. Ap.*, **99**, 218.
Savage, B. D., and Mathis, J. S. 1979, *Ann. Rev. Astr. Ap.*, **17**, 73.
Seaton, M. J., 1978, *M.N.R.A.S.*, **185**, 5p.
Shields, G. A., Aller, L. H., Keyes, C. D., and Czyzak, S. J., 1981, *Ap. J.*, **248**, 569.
Storey, P. J. 1981, *M.N.R.A.S.*, **195**, 27p.
Torres-Peimbert, S., and Peimbert, M. 1977, *Rev. Mexicana Astr. Ap.*, **2**, 181.
Torres-Peimbert, S., Peimbert, M., and Daltabuit, E. 1980*a*, *Ap. J.*, **238**, 133.
Torres-Peimbert, S., and Peña, M. 1981, *Rev. Mexicana Astr. Ap.*, **6**, 301.
Torres-Peimbert, S., Peña, M., and Daltabuit, E. 1980*b*, *The Universe at Ultraviolet Wavelengths*: *The First Two Years of IUE*, ed. R. D. Chapman (NASA Conf. Pub., No. 2171), p. 641.
Webster, B. L. 1984, *Proc. Astr. Soc. Australia*, **5**, 535.
Whitford, A. E. 1958, *A.J.*, **63**, 201.

JAMES B. KALER: Astronomy Department, University of Illinois, 349 Astronomy Building, 1011 West Springfield Avenue, Urbana, IL 61801